**INTERNATIONAL JOURNAL OF OPTIMIZATION IN CIVIL ENGINEERING**
***Int. J. Optim. Civil Eng., 2013; 3(4):673-693***

# APPLICATION OF ADAPTIVE NEURO-FUZZY INFERENCE SYSTEM FOR THE ASSESSMENT OF DAMAGED ZONE AROUND UNDERGROUND SPACES

H. Fattahi[1], S. Shojaee[*, †, 2] and M. A. Ebrahimi Farsangi[3]
[1]*Department of Mining Engineering, Arak University of Technology, Arak, Iran*
[2]*Department of Civil Engineering, Shahid Bahonar University of Kerman, Iran*
[3]*Department of Mining Engineering, Shahid Bahonar University of Kerman, Iran*

## ABSTRACT

The development of an excavation damaged zone (EDZ) around an underground excavation can change the physical, mechanical and hydraulic behaviors of the rock mass near an underground space. This might result in endangering safety, achievement of costs and excavation planed. This paper presents an approach to build a prediction model for the assessment of EDZ, based upon rock mass characteristics changed. Rock engineering systems (RES) was used as an appropriate method for choosing the best parameter that expresses the occurrence of EDZ. Modulus of deformation with the highest weight in the system was selected as the most effective changed parameter. The adaptive network-based fuzzy inference system (ANFIS) with modulus of deformation as input was used to build a prediction model for the assessment of EDZ. Three ANFIS models were implemented, grid partitioning (GP), subtractive clustering method (SCM) and fuzzy c-means clustering method (FCM). A comparison was made between these three models and the results show the superiority of the ANFIS-SCM model. Furthermore, a case study in a test gallery of the Gotvand dam, Iran was carried out to illustrate the capability of the ANFIS model defined.

Received: 20 September 2013; Accepted: 25 November 2013

KEY WORDS: excavation damaged zone, ANFIS, modulus of deformation, RES

[*]Corresponding author: S. Shojaee, Department of Civil Engineering, Shahid Bahonar University of Kerman, Iran
[†]E-mail address: saeed.shojaee@uk.ac.ir (S. Shojaee)

## 1. INTRODUCTION

The excavation of tunnel by blasting creates a zone of damaged rock around the tunnel in which the physical, mechanical and hydraulic properties of the rock zone immediately surrounding the excavation are changed. This zone is usually referred to as the excavation damaged zone. The disturbance and damage are mainly in the form of creation of new fractures, closure and opening of pre-existing fractures [1], and disturbance of the in situ stress [2]. Due to reduction of mechanical characteristics and increase in hydraulic properties (Figure 1), significant effects on the global behavior of the near-field rock mass and thus the overall performance of an excavation occur. The presence of this zone can pose problems related to stability and seepage and consequently impair the performance and functionality of the excavation [3]. Therefore, the understanding of the EDZ is essential for the optimal design of rock support. Furthermore, for support interaction studies at underground spaces, the mechanical properties of the EDZ, particularly those relating to deformation modulus are important.

Various researches about the assessment of EDZ with different methods such as displacement measurement, seismic refraction, direct observation, using borehole cameras, numerical methods were carried out worldwide. Geophysical methods were extensively used in the investigation of EDZ in various projects [4-6]. These methods are mostly based on seismic velocity measurements, which enable a non-invasive investigation of a large volume of rock around an excavation [7, 8]. Acoustic emission monitoring was also used to quantify and localize the rock mass damage and in particular to follow the EDZ evolution during an excavation process [9]. Geo-electric methods in indurate clay rocks [10] and radar reflection survey in crystalline rock mass [11] were also employed. All these geophysical methods that yield quantitative results are most often used in conjunction with each other [12, 13] and with other techniques such as visual inspection [14], core drilling analysis [15], fluorescence-doped resin injection prior to over core [16] that this method allows very detailed interpretation and identification of open fractures in the EDZ, estimates the in situ aperture and can provide information on the connectivity of fractures.

Hydraulic and pneumatic methods including hydraulic conductivity measurements; gas injection or extraction tests in boreholes; constitute a localized invasive means to delineate the EDZ and to estimate its transport properties. Different researches were carried out using such methods [17, 18].

Furthermore, the technique known as Adaptive Neuro-Fuzzy Inference System (ANFIS) seems to be suited successfully to model complex problems where the relationship between the model variables is unknown [19]. ANFIS was used by various researchers worldwide [20-22].

## 2. DEFINITIONS OF DAMAGED AND DISTURBED ZONES

Different definitions and names for the damaged and disturbed zones have been used. The EDZ is generally defined as the zone beyond the excavation boundary where, the rock has been considerably disturbed and/or damaged due to the excavation and re-distribution of stresses [23]. In this paper, the definitions of Tsang et al. [2] are used, which are described

as follows:

• The excavation disturbed zone (EdZ) is a zone with hydro-mechanical and geochemical modifications, without major changes in flow and transport properties. In the EdZ there are no negative effects on the long-term safety.

• The excavation damaged zone (EDZ) is a zone with hydro-mechanical and geochemical modifications inducing significant changes in flow and transport properties.

In addition, in this paper, a highly damaged zone (HDZ) is defined as a zone where, macro-scale fracturing or spalling may occur. The HDZ is part of the EDZ (Figure 1).

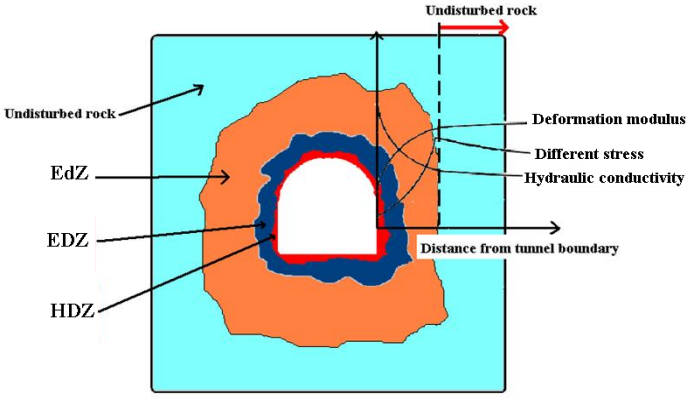


Figure 1. Various zones around an underground excavation

## 3. ROCK ENGINEERING SYSTEMS

The RES was established by Hudson in 1992 [24] and used by researchers worldwide [25-30]. It is a method, which has the capability of simultaneous analysis of relations among effective parameters of rock mass, site or structure, and discusses their interactions. For rock mechanics modeling and rock engineering design for a specific project, it is needed to be able to identify the relevant physical variables and the linking mechanisms, and then consider their combined operation. It is important to ensure that all the relevant factors and their interactions will be taken into account [24]. An RES description of the overall interactive mechanisms in drill and blasting operation seems to be an appropriate approach for choosing the best parameter among physical, mechanical and hydraulic parameters that have been changed due to a blasting impact and stress redistribution after excavation. The selected parameter can be used for the assessment of EDZ.

### *3.1 The Interaction Matrix and Its Coding*

Interaction matrix is the basic device used by the rock engineering systems. A systematic method for thinking about all the interactions is to list them in a matrix. The principal parameters considered relevant to the problem are listed along the leading diagonal of a square matrix from top left to bottom right and the interactions between pairs of principal parameters form the off-diagonal terms [24]. The off-diagonal terms, are assigned values, which describe the degree of the influence of one factor (or parameter) on the other factor

(or parameter) (Figure 2). Assigning these values is called coding the matrix. Several methods have been presented for numerically coding this matrix such as binary method, the expert semi-quantitative (ESQ) method [24] and the continuous quantitative coding (CQC) method [31]. Among these methods, the ESQ method is the most widely used, which is shown in Table 1. The sum of each row is the "cause" value and the sum of each column is the "effect" value, designated as coordinates (C, E) for each particular parameter. These procedures are shown in Figure 2. The result of comprising such a matrix is a table including useful information about the interactive intensity (C+E) and dominance (C-E) (Table 2). The percentage value of (C+E) can be used as the parameter's weighting factor ($a_i$), as shown in Eq. (1):

$$a_i = \frac{(C_i + E_i)}{(\sum C_i + \sum E_i)} \times 100 \tag{3}$$

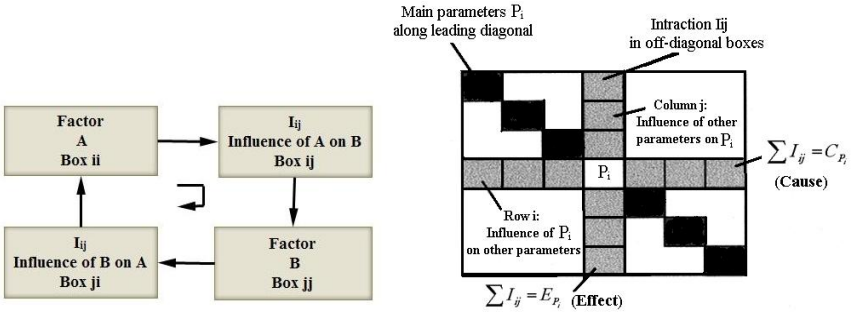


Figure 2. Illustration of the interaction matrix (after [24]).

Table 1: Code number concepts [24]

| **Code number** | Concept |
|---|---|
| **0** | No interaction |
| **1** | Weak interaction |
| **2** | Medium interaction |
| **3** | Strong interaction |
| **4** | Critical interaction |

Table 2: Result of an interaction matrix

| **Parameters** | C | E | C+E | C-E | $a_i$ |
|---|---|---|---|---|---|
| **$P_1$** | $C_1$ | $E_1$ | $C_1$+ $E_1$ | $C_1$- $E_1$ | $a_1$ |
| **$P_2$** | $C_2$ | $E_2$ | $C_2$+ $E_2$ | $C_2$- $E_2$ | $a_2$ |
| **$P_3$** | $C_3$ | $E_3$ | $C_3$+ $E_3$ | $C_3$- $E_3$ | $a_3$ |
| . | . | . | . | . | . |
| . | . | . | . | . | . |

## 4. CHOOSING THE BEST PARAMETER FOR ASSESSMENT OF EDZ, USING THE RES

The identified 11 parameters, which can be changed by impact of blasting and stress redistribution after excavation are illustrated in Table 3. These parameters are listed along the leading diagonal of a square matrix, the interaction matrix. The interaction matrix coding was carried out based upon the views of 3 experts, using the ESQ coding and the results obtained are shown in Figure 3.

Table 3: The main physical, mechanical and hydraulic parameters, changed after excavation

| No. | Parameters |
|---|---|
| **P1** | RQD |
| **P2** | Uniaxial compressive strength |
| **P3** | Permeability |
| **P4** | Cohesion |
| **P5** | Internal friction angle |
| **P6** | Deformation modulus |
| **P7** | Wave velocity |
| **P8** | Effective porosity |
| **P9** | Poisson's ratio |
| **P10** | Specific gravity |
| **P11** | Brazilian tensile strength |

| | | | | | | | | | | |
|---|---|---|---|---|---|---|---|---|---|---|
| **P1** | 1 | 2 | 1 | 1 | 2 | 2 | 1 | 1 | 1 | 1 |
| **2** | P2 | 2 | 2 | 2 | 3 | 3 | 1 | 2 | 3 | 2 |
| **1** | 1 | P3 | 1 | 1 | 2 | 2 | 2 | 1 | 1 | 1 |
| **2** | 2 | 2 | P4 | 2 | 2 | 2 | 2 | 1 | 1 | 2 |
| **1** | 2 | 1 | 2 | P5 | 2 | 2 | 1 | 1 | 1 | 2 |
| **3** | 3 | 3 | 3 | 3 | P6 | 3 | 1 | 3 | 3 | 3 |
| **2** | 3 | 2 | 1 | 1 | 3 | P7 | 2 | 2 | 2 | 2 |
| **1** | 2 | 3 | 1 | 1 | 2 | 1 | P8 | 1 | 2 | 2 |
| **1** | 3 | 1 | 2 | 2 | 3 | 2 | 1 | P9 | 1 | 2 |
| **1** | 2 | 2 | 1 | 1 | 2 | 2 | 1 | 1 | P10 | 2 |
| **2** | 2 | 2 | 1 | 1 | 2 | 2 | 1 | 2 | 2 | P11 |

Figure 3. Illustration of the interaction matrix coding results

The benefit of comprising an interaction matrix is the understanding of the interaction of parameters, which are assumed to have considerable influence on the assessment of EDZ. The results obtained helps finding the most representative parameter, which can be used for the assessment of EDZ. Weight of each parameter represents the degree of interactive intensity in the system. As it is shown in Table 4 and Figure 4, deformation modulus has the highest weight in the system, which controls other elements. Thus, the modulus of

deformation is the best parameter among other parameters that represents the behavior of rock mass after excavation, which can be used for the assessment of EDZ.

Table 4: The results of comprising interaction matrix for selecting the best parameter

| No. | Parameters | C | E | C+E | C-E | $a_i$ (%) |
|---|---|---|---|---|---|---|
| **1** | RQD | 13 | 16 | 29 | -3 | 7.44 |
| **2** | Uniaxial compressive strength | 22 | 21 | 43 | 1 | 11.03 |
| **3** | Permeability | 13 | 20 | 33 | -7 | 8.46 |
| **4** | Cohesion | 18 | 15 | 33 | 3 | 8.46 |
| **5** | Internal friction angle | 15 | 15 | 30 | 0 | 7.69 |
| **6** | Deformation modulus | 28 | 23 | 51 | 5 | 13.08 |
| **7** | Wave velocity | 20 | 21 | 41 | -1 | 10.51 |
| **8** | Effective porosity | 16 | 13 | 29 | 3 | 7.44 |
| **9** | Poisson's ratio | 18 | 15 | 33 | 3 | 8.46 |
| **10** | Specific gravity | 15 | 17 | 32 | -2 | 8.21 |
| **11** | Brazilian tensile strength | 17 | 19 | 36 | -2 | 9.23 |
| | **Sum** | 195 | 195 | 390 | 0 | 100 |

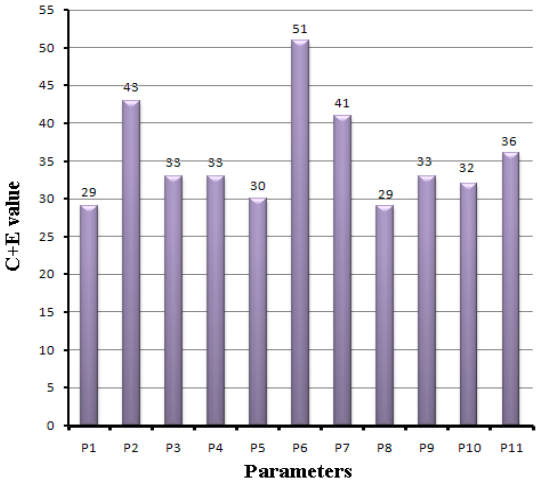


Figure 4. The histogram for C+E

## 5. FIELD STUDY

### *5.1 Site Descriptions and Geology*

The Gotvand dam is located on the Karun river in the Khuzestan province, south west of Iran. This dam with 178 m height and 730 m length of embankment, regulates the water of the Karun river, also serves power generation, flood control and irrigation needs [32]. The geology of area consists of two formations; Bakhtiary (BK) and Aghajari (AJ). The BK formation is composed of conglomerate, cherty limestone and inter bedded mudstones and

sandstone. The conglomerate mainly consists of limestone pebbles but it also contains a significant amount of fragments. This formation is of upper Pliocene age that overlies the AJ formation .

The AJ formation contains 2 to 5 m thick layers of gray and greenish gray sandstones, inter bedded claystone, siltstone and brow reddish marlstone. More resistant than the fine-grained, the sandstone usually forms topographic heights and steep benches alternating with gentler slopes corresponding to the softer inter bedds. The sandstones of the AJ formation are composed of the well-rounded siliceous-limy grains with approximately 70% lime and 30% quartz. The AJ formation, of late Miocene to lower Pliocene age, overlies the Mishan formation [32].

Around the Gotvand dam, four galleries were excavated by drill and blast, three in the right bank (galleries A, C and D), and one in the lower part of the left bank (gallery B), to carry out the in situ tests. As deformation modulus is reduced in the EDZ (Figure1), plate loading tests were performed in galleries to determine deformation modulus for the assessment of EDZ.

### *5.2 Plate loading Test for Determination of Deformation Modulus*

The plate loading test (PLT) is the most familiar in situ experiment in rock mass studying. It is generally conducted in special test galleries or underground spaces excavated by conventional drill and blast, having a span of 2 m and a height of 2.5 m. In the PLT, load is directly imposed on the wall of gallery, and the resultant displacement is measured on the loading point in rock. A cycle of loading and unloading (Figure 5) provides the load-displacement curve, which is necessary to deformation modulus determination [33].

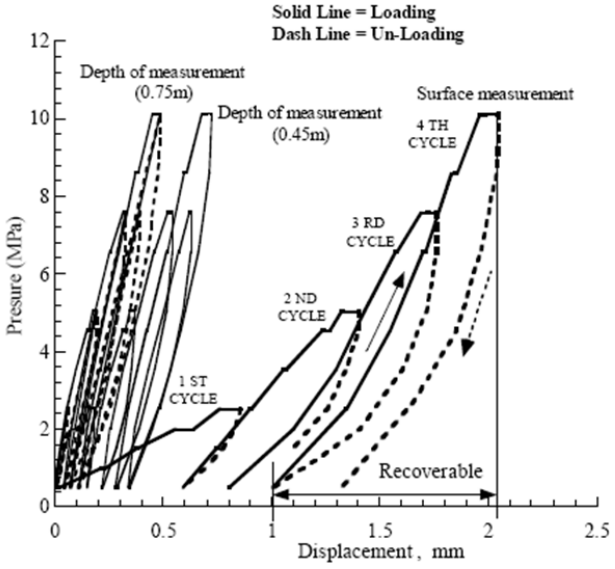


Figure 5. Pressure-displacement curves obtained from the PLT [33].

The recoverable displacement is used to evaluate the deformation modulus based on the theory of elasticity. Depending on the loading condition, the PLT can be classified into a

flexible type and a rigid type. In this paper, the flexible PLT procedure suggested by the ISRM 1981 in which Boussinesq's equation is applied in the interpretation of the PLT results is used. The fundamental set-up of the PLT is illustrated in Figure 6.

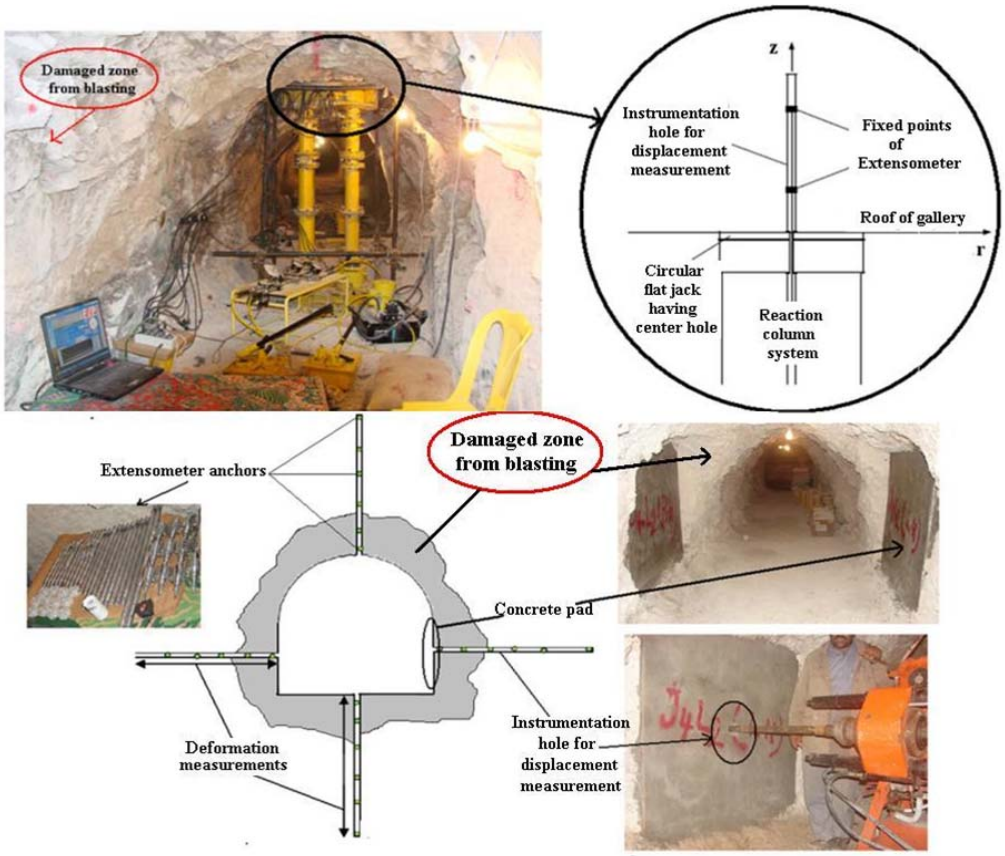


Figure 6. The set-up of PLT

In the following, to show the formulation, the cylindrical coordinates system ($r, \theta, z$) is used and the displacement components are represented by ($u, v, w$), respectively. It is assumed that the total force ($P$) is applied perpendicular to the plane of $z = 0$, and the displacement component ($w$) in the $z$ direction is measured. The flexible plate loading test gives the uniform pressure ($p$) in a circular area of radius a, and the resultant displacement ($w$) is measured in boreholes behind loaded surface by utilizing extensometers, which can provide the relative displacement at different depths . Thus the test procedure consists of preparation of the test site, drilling the instrumentation hole, installation of the extensometer, adjustment of the loading system, imposing the uniform pressure, measuring the rock deformation, recording the data, and subsequent data processing. The displacement ($w$) is usually measured along the center axis of $r = 0$, which can be formulated as a function of the uniform pressure ($p$) . In the case that the pressure ($p$) is given in a circular area of radius $r < a$, the normalized displacement ($w/a$) is written as follows:

$$\frac{w}{a} = p.\frac{(1+\nu)}{E}.\Phi_1(\zeta) + p.\frac{(1-\nu^2)}{E}.\Phi_2(\zeta) \tag{2}$$

By introducing two functions of dimensionless:

$$\Phi_1(\zeta) = \zeta - \frac{\zeta^2}{\sqrt{1+\zeta^2}}, \Phi_2(\zeta) = 2(\sqrt{1+\zeta^2} - \zeta),\ \ \zeta = \frac{z}{a} \tag{3}$$

where, $E$, $\nu$ are the deformation modulus and Poisson's ratio respectively. Therefore the maximum displacement ($w_{max}$) appears at the center of loaded area, which is given by:

$$\frac{w_{\max}}{a} = p.\frac{2(1-\nu^2)}{E} \tag{4}$$

In the general case, which the pressure ($p$) is given in a circular area of radius $b < r < a$, avoiding the instrumentation hole, the normalized displacement ($w/a$) is written as follows:

$$\frac{w}{a} = \frac{p}{E}.K(\zeta_a, \zeta_b) \tag{5}$$

where,

$$\begin{aligned} K(\zeta_a, \zeta_b) &= (1+\nu).\Omega_1(\zeta_a, \zeta_b) + (1-\nu^2).\Omega_2(\zeta_a, \zeta_b) \\ \Omega_k(\zeta_a, \zeta_b) &= \Phi_k(\zeta_a) - \frac{b}{a}.\Phi_k(\zeta_b)\ ,\ \zeta_a = \frac{z}{a},\ \zeta_b = \frac{z}{b}. \end{aligned} \tag{6}$$

The relative displacement ($\Delta w$) measured by the extensometer is formulated as follows:

$$\frac{\Delta w}{a} = \frac{w_i - w_j}{a} = \frac{p}{E}.\left[K(\zeta_a^i, \zeta_b^i) - K(\zeta_a^j, \zeta_b^j)\right] \tag{7}$$

where,

$$\zeta_a^i = \frac{z_i}{a}\ ,\ \zeta_b^j = \frac{z_j}{b} \tag{8}$$

In these equations, the subscript ($i$ and $j$) of w and the superscript ($i$ and $j$) of $z$ represent the number of displacement measurement by the extensometer .

## 6. ADAPTIVE NEURO-FUZZY INFERENCE SYSTEM

A fuzzy inference system can model the qualitative aspects of human knowledge and reasoning processes without employing precise quantitative analyses. Neural networks (NN) are information-processing programs inspired by mammalian brain processes. NN are composed of a number of interconnected processing elements analogous to neurons. The training algorithm inputs to the NN a set of input data and checks the NN output desired result. Combining neural networks with fuzzy logic has been shown to emulate the human process of expert decision-making reasonably. In traditional NN, only weight values change during learning, therefore the learning ability of neural networks is combined with the inference mechanism of fuzzy logic for a neuro-fuzzy decision-making system [34].

An adaptive neural network is a network structure consisting of several nodes connected through directional links. Each node is characterized by a node function with fixed or adjustable parameters. Once the fuzzy inference system is initialized, neural network algorithms can be used to determine the unknown parameters (premise and consequent parameters of the rules) minimizing the error measure, as conventionally defined for each variable of the system. Due to this optimization procedure the system is called adaptive. An adaptive network is presented in Figure 7a, which is functionally equivalent to a fuzzy inference system in Figure 7b.

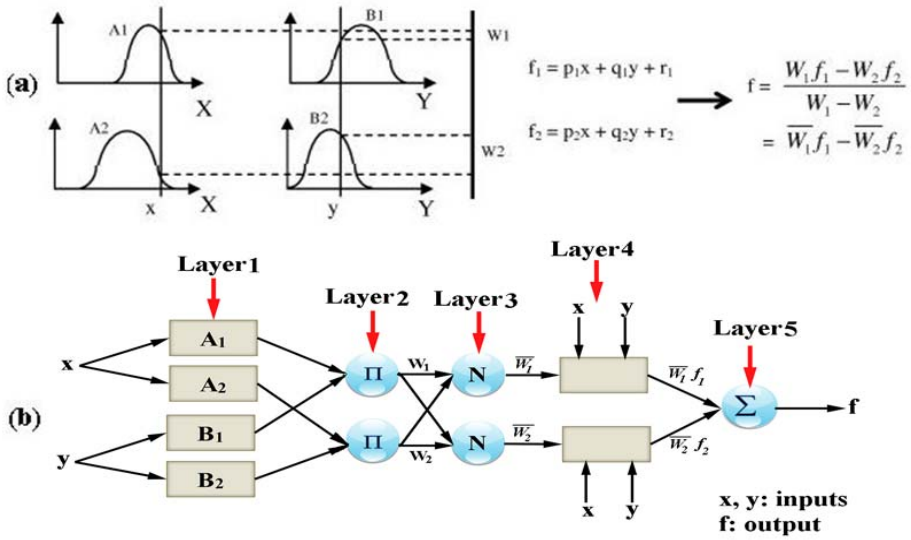


Figure 7. a The first-order of Takagi– Sugeno–Kang (TSK) fuzzy model, b Corresponding ANFIS architecture (after [35])

In practice, a neural fuzzy model is used [36], which consists of five layers:

Layer 1: each node *i* in this layer generates a membership grades of a linguistic label. For instance, the node function of the $i^{th}$ node might be:

$$Q_i^1 = \mu_{Ai}(x) = \frac{1}{1+\left[\left(\frac{x-v_i}{\sigma_i}\right)^2\right]^{b_i}} \tag{9}$$

where, $x$ is the input to node i, and Ai is the linguistic label (small, large, …) associated with this node; and $\{\sigma_i, V_i, b_i\}$ is the parameter set that changes the shapes of the membership function. Parameters in this layer are referred to as the "premise parameters".

Layer 2: Each node in this layer calculates the "firing strength" of each rule via multiplication:

$$Q_i^2 = W_i = \mu_{Ai}(x).\mu_{Bi}(y) \quad i = 1,2 \tag{10}$$

Layer 3: The $i^{th}$ node of this layer calculates the ratio of the $i^{th}$ rule's firing strength to the sum of all rules' firing strengths:

$$Q_i^3 = \bar{W}_i = \frac{w_i}{\sum_{j=1}^{2} w_j}, \quad i = 1,2 \tag{11}$$

For convenience, outputs of this layer will be called "normalized firing" strengths.

Layer 4: Every node $i$ in this layer is a node function:

$$Q_i^4 = \bar{W}_i f_i = \bar{W}_i (p_i x + q_i y + r_i) \tag{12}$$

where, $\bar{W}_i$ is the output of layer 3. Parameters in this layer will be referred to as "consequent parameters".

Layer 5: The single node in this layer is a circle node labeled R that computes the "overall output" as the summation of all incoming signals:

$$Q_i^5 = Overall\ Output = \sum \bar{W}_i f_i = \frac{\sum w_i f_i}{\sum w_i} \tag{13}$$

For a given data set, different ANFIS models can be constructed, using different identification methods. Grid partitioning (GP), Subtractive clustering method (SCM) and Fuzzy C-means clustering method (FCM) are three methods used in this paper to identify the antecedent membership functions.

### *6.1 Grid Partitioning of the Antecedent Variables*

This method proposes independent partitions of each antecedent variable [35]. The expert developing the model can define the membership functions of all antecedent variables using

prior knowledge and experience. They are designed to represent the meaning of the linguistic terms in a given context. However, for many systems no specific knowledge is available on these partitions. In that case, the domains of the antecedent variables can simply be partitioned into a number of equally spaced and equally shaped membership functions. Therefore, in the grid partitioning method, the domain of each antecedent variable is partitioned into equidistant and identically shaped membership functions. Using the available input-output data, the parameters of the membership functions can be optimized.

*6.2 Subtractive Clustering Method*

Subtractive clustering method proposed by Chiu [37] in which data points are considered as the candidates for center of clusters. The algorithm continues as follow:

At first a collection of n data points $\{X_1, X_2, X_3, ..., X_n\}$ in an M-dimensional space is considered. Since each data point is a candidate for cluster center, a density measure at data point $X_i$ is defined as:

$$D_i = \sum_{j=1}^{n} \exp\left( -\frac{\left\| x_i - x_j \right\|^2}{\left( \frac{r_a}{2} \right)^2} \right) \tag{14}$$

where, $r_a$ is a positive constant. Hence, a data point will have a high density value if it has many neighboring data points. The radius $r_a$ defines a neighborhood; data points outside this radius contribute only slightly to the density measure. After the density measure of each data point has been calculated, the data point with the highest density measure is selected as the first cluster center. Let $X_{c1}$ be the point selected and $D_{c1}$ its density measure. Next, the density measure for each data point $x_i$ is revised as follows:

$$D_i = D_i - D_{ci} \exp\left( -\frac{\left\| x_i - x_{ci} \right\|^2}{\left( \frac{r_b}{2} \right)^2} \right) \tag{15}$$

where, $r_b$ is a positive constant. After the density calculation for each data point is revised, the next cluster center $X_{c2}$ is selected and all of the density calculations for data points are revised again. This process is repeated until a sufficient number of cluster centers are generated.

*6.3 Fuzzy C-means Clustering Method*

Fuzzy C-means method is a data clustering algorithm proposed by Bezdek [38] in which each data point belongs to a cluster to a degree specified by a membership grade. FCM partitions a collection of n vector $X_i$, $i=1,2,...,n$, into C fuzzy groups, and finds a cluster center in each group such that a cost function of dissimilarity measure is minimized. The stages of FCM algorithm are therefore, first described in brief. At first, the cluster centers $c_i$, $i=1,2,...,C$ randomly from the n points $\{X_1, X_2, X_3, ..., X_n\}$ is choosen. After that the membership matrix U using the following equation is computed:

$$\mu_{ij} = \frac{1}{\sum_{k=1}^{c} (\frac{d_{ij}}{d_{kj}})^{2/m-1}} \tag{16}$$

where, $d_{ij} = \|c_i - x_j\|$ is the Euclidean distance between $i^{th}$ cluster center and $j^{th}$ data point, and *m* is the fuzziness index. Then, the cost function according to the following equation is computed. The process is stopped if it is below a certain threshold.

$$J(U, c_1, ..., c_2) = \sum_{i=1}^{c} J_i = \sum_{i=1}^{c} . \sum_{j=1}^{n} \mu_{ij}^m d_{ij}^2 \tag{17}$$

In final step, a new c fuzzy cluster centers $c_i$, $i=1,2,...,C$ using the following equation is computed:

$$c_i = \frac{\sum_{j=1}^{n} \mu_{ij}^m x_j}{\sum_{j=1}^{n} \mu_{ij}^m} \tag{18}$$

## 7. PREDICTION OF DEFORMATION MODULUS USING, ANFIS MODEL

In this paper, the GP, SCM and FCM are applied to model the EDZ, using MATLAB environment. Figure 8 shows the fuzzy architecture of the ANFIS. As it can be seen in Figure 8, X, Y and Z coordinates (location of installation extensometers from the portal of test gallery that in these points, displacements and modulus of deformations are obtained) were introduced as input parameters into the ANFIS models and deformation modulus as output. The proposed models were trained with 80 data sets obtained from a test gallery in the Gotvand dam for training phase. The 10 samples of training data sets are shown in Table 5.


Figure 8. Architecture of the ANFIS based on the GP, SCM and FCM

Table 5: Samples of the training data sets used for learning the ANFIS

| No. | Depth of extensometer in instrumentation hole (m) | Input | | | Output |
|---|---|---|---|---|---|
| | | X (m) | Y (m) | Z (m) | Deformatin modulus (GPa) |
| 1 | 0.5 | 6 | 7.75 | 3 | 3.18 |
| 2 | 1 | 6 | 8.25 | 3 | 6.48 |
| 3 | 0.4 | 7.65 | 6 | 9 | 7.75 |
| 4 | 1.2 | 8.45 | 6 | 9 | 14.9 |
| 5 | 0.4 | 7.65 | 6 | 27 | 4.3 |
| 6 | 0 | 6 | 7.25 | 9 | 2.11 |
| 7 | 0.9 | 6 | 3.85 | 27 | 9.42 |
| 8 | 2.3 | 9.55 | 6 | 3 | 24.95 |
| 9 | 0.4 | 7.65 | 6 | 27 | 4.32 |
| 10 | 0.5 | 6 | 4.25 | 9 | 3.33 |

The characterizations of the ANFIS models are revealed in Table 6.

Table 6: Characterizations of the ANFIS models

| ANFIS parameter | ANFIS (GP) | ANFIS (SCM) | ANFIS (FCM) |
|---|---|---|---|
| Membership function type | Gaussian | Gaussian | Gaussian |
| Output membership function | Linear | Linear | Linear |
| Number of nodes | 110 | 262 | 86 |
| Number of linear parameters | 52 | 128 | 120 |
| Number of nonlinear parameters | 78 | 192 | 20 |
| Total number of parameters | 130 | 320 | 140 |
| Number of training data pairs | 80 | 80 | 80 |
| Number of testing data pairs | 19 | 19 | 19 |
| Number of fuzzy rules | 13 | 32 | 30 |

The number of rules obtained for the GP, SCM and FCM models are 13, 32 and 30 respectively. The membership functions (MF) of the input parameters for different models are shown in Figure 9.

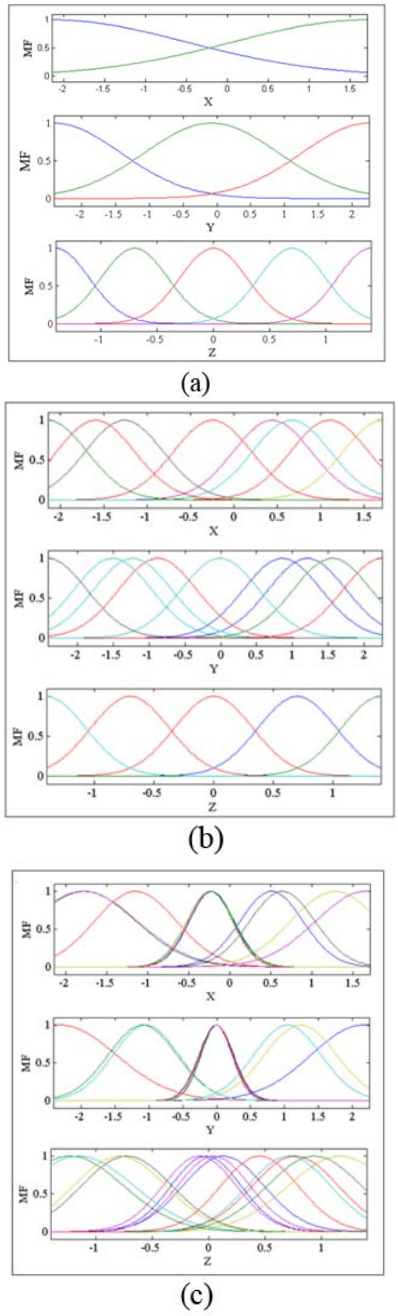


Figure 9. Membership functions obtained: (a) GP, (b) SCM, (c) FCM

To evaluate the performances of the ANFIS models, the variance account for (VAF) ( Eq. (19)) and the root mean square error (RMSE) (Eq. (20)) indices with 19 sets of data were used. A few samples of data sets for testing are presented in Table 7.

Table 7: Samples for testing the ANFIS models

| No. | Depth of extensometer in instrumentation hole (m) | Input | | | Output |
|---|---|---|---|---|---|
| | | X (m) | Y (m) | Z (m) | Deformation modulus (GPa) |
| 1 | 0 | 6 | 7.25 | 3 | 0.955 |
| 2 | 0.6 | 4.15 | 6 | 3 | 9.274 |
| 3 | 0.9 | 6 | 3.85 | 3 | 2.55 |
| 4 | 0.5 | 6 | 7.75 | 27 | 3.829 |
| 5 | 1.2 | 3.55 | 6 | 27 | 9.66 |

$$VAF = \left(1 - \frac{\text{var}(y - y')}{\text{var}(y)}\right) \tag{19}$$

$$RMSE = \sqrt{\frac{1}{N}\sum_{i=1}^{N}(y - y')^2} \tag{20}$$

where, *var* denotes the variance, y and $y'$ are the measured and predicted values, respectively, and N is the number of samples. The higher the VAF, the better is the model performance. For instance, a VAF of 100% means that the measured output has been predicted exactly (perfect model). VAF=0 means that the model performs as poorly as a predictor using simply the mean value of the data. Also, the lower RMSE indicates the better performance of the model. In addition, the determination coefficient ($R^2$) is calculated. Figure 10 illustrates the correlation between measured and predicted values of the deformation modulus for three ANFIS models.

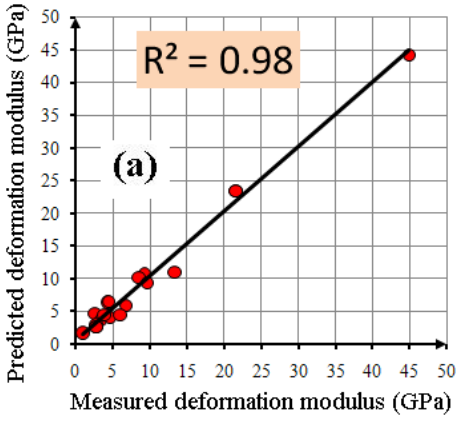

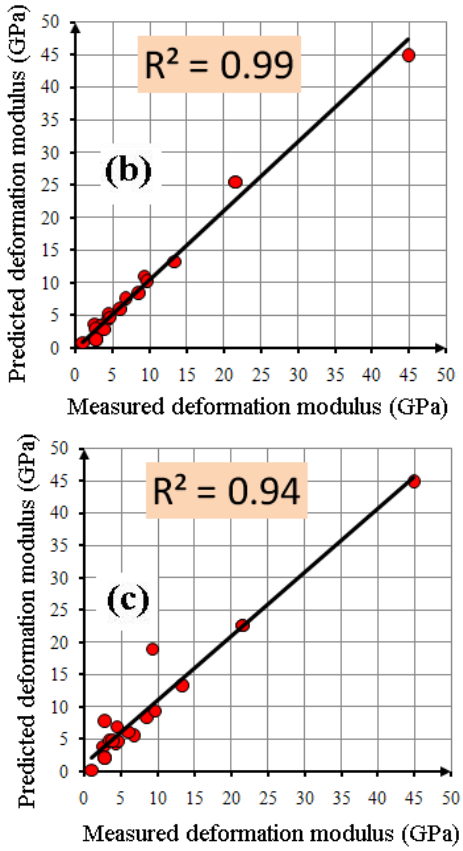


Figure 10. Correlation between measured and predicted values of deformation modulus: (a) GP, (b) SCM, (c) FCM

A comparison between the results of three models is shown in Table 8. As it can be observed from this table, the SCM model with $R^2$= 0.99, VAF= 98.10 and RMSE = 1.49 performs better than the other two models for the modeling of EDZ.

Table 8: A comparison between the results of three models

| ANFIS model | RMSE | VAF | $R^2$ |
|---|---|---|---|
| ANFIS (GP) | 1.68 | 97.45 | 0.98 |
| ANFIS (SCM) | 1.49 | 98.10 | 0.99 |
| ANFIS (FCM) | 3.65 | 87.03 | 0.94 |

SCM with the best performance was selected to assess the potential of creating the EDZ and HDZ around a test gallery in the Gotvand dam. For instance, the EDZ and HDZ around 6-section with different distances (Z = 3 m, Z = 5m, Z = 10 m, Z = 12 m, Z = 16 m and Z = 22 m) from the portal of the gallery were obtained, as shown in Figure 11. In these sections, the data generating (random (x,y,z)) was carried out, using MATLAB environment. The

modulus of deformation for rock mass in the Gotvand dam is 5.8 GPa [39]. As the EdZ is a zone without major changes in flow and transport properties [2] and there are no negative effects on the long-term safety [40], a modulus of deformation of 5 GPa is assumed for this zone. Also, a threshold of less than 2 GPa was chosen to recognize the HDZ, which is a part of EDZ.

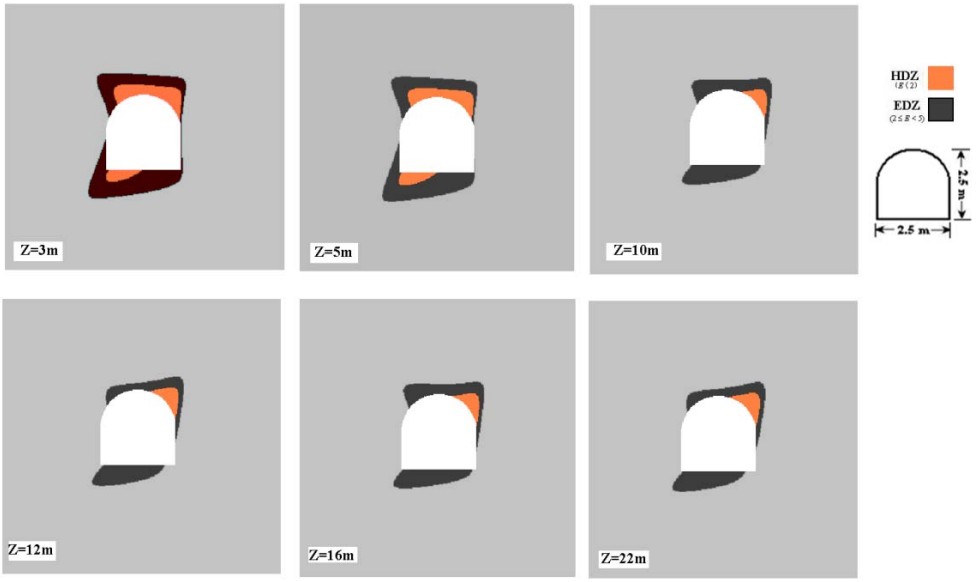


Figure 11. The EDZ and HDZ around different sections of a gallery, Gotvand dam

In Figure 11, the orange region shows HDZ ($E\langle 2$), while the black region is EDZ ($2 \le E\langle 5$). According to the results of ANFIS modeling, the EDZ at the test gallery around the Gotvand dam extends approximately 0.5-1 m into the rock mass. Also, variation of deformation modulus of the EDZ is approximately 26-83% of the undisturbed rock, since the minimum and maximum values for the black and grey regions are 1.01 GPa and 4.32 GPa respectively.

## 6. CONCLUSIONS

In this paper a new approach for the assessment of EDZ was proposed and the following remarks were concluded:

- Using the RES, among the 11 effective parameters on the EDZ, deformation modulus was selected as the best parameter for the assessment of EDZ.
- A comparison was made between three ANFIS models, GP, SCM and FCM, using the PLT measurements, and based upon the performance indices; $R^2$, RMSE and VAF, SCM with $R^2$= 0.99, RMSE= 1.49 and VAF= 98.10 was selected as the best predictive model.
- Based upon the results of ANFIS-SCM modeling, the extent of the EDZ at the test gallery around Gotvand dam is approximately 0.5-1 m into the rock mass. Furthermore,

deformation modulus of the EDZ is approximately 26-83% of the undisturbed rock.

- The ANFIS-SCM modeling as a good tool can estimate the damage occurred due to blasting around each section of an underground excavation.

## REFERENCES


1. Sato T, Kikuchi T, Sugihara K. In-situ experiments on an excavation disturbed zone induced by mechanical excavation in Neogene sedimentary rock at Tono mine, central Japan, *Eng Geol*, 2000; **56**(1–2): 97-108.
2. Tsang CF, Bernier F, Davies C. Geohydromechanical processes in the Excavation Damaged Zone in crystalline rock, rock salt, and indurated and plastic clays-in the context of radioactive waste disposal, *Int J Rock Mech Min Sci*, 2005; **42**(1): 109-25.
3. Saiang D. *Behaviour of blast-induced damage zone around underground excavations in hard rock mass* [Ph.D. Thesis]. Lulea˚: Lulea˚University of Technology, Sweden, 2008.
4. Meglis IL, Chow T, Martin CD, Young RP. Assessing in situ microcrack damage using ultrasonic velocity tomography, *Int J Rock Mech Min Sci*, 2005; **42**(1): 25-34.
5. Lee SW, Park KH, Lee JG. Blast-induced damage identification of rock mass using wavelet transform analysis, *Procedia Eng*, 2011; **14**(0): 3142-6.
6. García Bastante F, Alejano L, González-Cao J. Predicting the extent of blast-induced damage in rock masses, *Int J Rock Mech Min Sci*, 2012; **56**(0): 44-53.
7. Nicollin F, Gibert D, Bossart P, Nussbaum C, Guervilly C. Seismic tomography of the excavation damaged zone of the gallery 04 in the Mont Terri rock laboratory, *Geophys J Int*, 2008; **172**(1): 226-39.
8. Shao H, Schuster K, Sönnke J, Bräuer V. EDZ development in indurated clay formations - In situ borehole measurements and coupled HM modelling, *Phys Chem Earth*, 2008; **33**, Supplement 1(0): S388-S95.
9. Suzuki K, Nakata E, Minami M, Hibino E, Tani T, Sakakibara J, et al. Estimation of the zone of excavation disturbance around tunnels, using resistivity and acoustic tomography, *Explor Geophys*, 2004; **35**(1): 62-9.
10. Nicollin F, Gibert D, Lesparre N, Nussbaum C. Anisotropy of electrical conductivity of the excavation damaged zone in the Mont Terri underground rock laboratory, *Geophys J Int*, 2010; **181**(1): 303-20.
11. Kwon S, Lee CS, Cho SJ, Jeon SW, Cho WJ. An investigation of the excavation damaged zone at the KAERI underground research tunnel, *Tunn Undergr Sp Tech*, 2009; **24**(1): 1-13.
12. Falls SD, Young RP. Acoustic emission and ultrasonic-velocity methods used to characterise the excavation disturbance associated with deep tunnels in hard rock, *Tectonophysics*, 1998; **289**(1–3): 1-15.
13. Cosma C, Olsson O, Keskinen J, Heikkinen P. Seismic characterization of fracturing at the Äspö Hard Rock Laboratory, Sweden, from the kilometer scale to the meter scale, *Int J Rock Mech Min Sci*, 2001; **38**(6): 859-65.

14. Martini CD, Read RS, Martino JB. Observations of brittle failure around a circular test tunnel, *Int J Rock Mech Min Sci*, 1997; **34**(7): 1065-73.
15. Bossart P, Thury M. *Mont Terri rock laboratory project, programme 1996 to 2007 and results, rep*. Swiss geological survey 3. Wabern, Switzerland, 2008.
16. Bossart P, Trick T, Meier PM, Mayor JC. Structural and hydrogeological characterisation of the excavation-disturbed zone in the Opalinus clay (Mont Terri Project, Switzerland), *Appl Clay Sci*, 2004; **26**(1–4): 429-48.
17. Levasseur S, Charlier R, Frieg B, Collin F. Hydro-mechanical modelling of the excavation damaged zone around an underground excavation at Mont Terri Rock Laboratory, *Int J Rock Mech Min Sci*, 2010; **47**(3): 414-25.
18. Kwon S, Cho WJ. The influence of an excavation damaged zone on the thermal-mechanical and hydro-mechanical behaviors of an underground excavation, *Eng Geol*, 2008; **101**(3–4): 110-23.
19. Cabalar AF, Cevik A, Gokceoglu C. Some applications of adaptive neuro-fuzzy inference system (ANFIS) in geotechnical engineering, *Comput Geotech*, 2012; **40**:14-33.
20. Yesiloglu-Gultekin N, Sezer E, Gokceoglu C, Bayhan H. An application of adaptive neuro fuzzy inference system for estimating the uniaxial compressive strength of certain granitic rocks from their mineral contents, *Expert Syst Appl*, 2012; **40**(3): 921–8.
21. Singh R, Vishal V, Singh T, Ranjith P. A comparative study of generalized regression neural network approach and adaptive neuro-fuzzy inference systems for prediction of unconfined compressive strength of rocks, *Neural Comput Appl*, 2013; **23**(2): 499-506.
22. Verma A, Singh T. A neuro-fuzzy approach for prediction of longitudinal wave velocity, *Neural Comput Appl*, 2013; **22**(7-8): 1685-93.
23. Bäckblom G, Martin CD. Recent experiments in hard rocks to study the excavation response: Implications for the performance of a nuclear waste geological repository, *Tunn Undergr Sp Tech*, 1999; **14**(3): 377-94.
24. Hudson JA. *Rock engineering systems : theory and practice*. Chichester: Horwood, 1992.
25. Cancelli A, Crosta G. *Hazard and risk assessment in rockfall prone areas*. In: Skipp B (ed) Risk and Reliability in Ground Engineering, Thomas Telford, London1993, pp. 177-190.
26. Mazzoccola D, Hudson J. A comprehensive method of rock mass characterization for indicating natural slope instability, *Q J Eng Geol*, 1996; **29**(1): 37-56.
27. Benardos A, Kaliampakos D. A methodology for assessing geotechnical hazards for TBM tunnelling—illustrated by the Athens Metro, Greece, *Int J Rock Mech Min Sci*, 2004; **41**(6): 987-99.
28. Shin HS, Kwon YC, Jung YS, Bae GJ, Kim YG. Methodology for quantitative hazard assessment for tunnel collapses based on case histories in Korea, *Int J Rock Mech Min Sci*, 2009; **46**(6): 1072-87.
29. Faramarzi F, Ebrahimi Farsangi M, Mansouri H. An RES-based model for risk assessment and prediction of backbreak in bench blasting, *Rock Mech Rock Eng*, 2013; **46**(4): 877-87.
30. Faramarzi F, Mansouri H, Ebrahimi Farsangi M. A rock engineering systems based model to predict rock fragmentation by blasting, *Int J Rock Mech Min Sci*, 2013; **60**:82-94.

31. Lu P, Latham JP. A continuous quantitative coding approach to the interaction matrix in rock engineering systems based on grey systems approaches. *Proc 7th Int Cong of IAEG*, Balkema, Rotterdam, 1994, pp. 4761-4770.
32. Moshanir, CAITEC. *Upper Gotvand hydroelectric power project*. Gotvand1997, p. 155.
33. Faramarzi L, Fattahi H. Interpretation of plate loading test results on major project. *5th Asian Rock Mechanics Symposium (ARMS5)*. Tehran, Iran, 2008, pp. 255-260.
34. Lin CT, Lee CSG. Neural-network-based fuzzy logic control and decision system, *IEEE T Comput*, 1991; **40**(12): 1320-36.
35. Jang JSR. ANFIS: Adaptive-network-based fuzzy inference system, *IEEE T Syst Man Cyb*, 1993; **23**(3): 665-85.
36. Zhou QQ, Purvis M, Kasabov N. A membership function selection method for fuzzy neural networks. *Proc ICONIP1997*, pp. 785-788.
37. Chiu SL. Fuzzy model identification based on cluster estimation, *Journal of intelligent and Fuzzy systems*, 1994; **2**(3): 267-78.
38. Bezdek JC. *Fuzzy mathematics in pattern classification*. Ithaca: Cornell university, 1973.
39. Bashari A, Beiki M, Talebinejad A. Estimation of deformation modulus of rock masses by using fuzzy clustering-based modeling, *Int J Rock Mech Min Sci*, 2011; **48**(8): 1224-34.
40. Blümling P, Bernier F, Lebon P, Derek Martin C. The excavation damaged zone in clay formations time-dependent behaviour and influence on performance assessment, *Phys Chem Earth*, 2007; **32**(8–14): 588-99.